Self-Segregation of Myelin Membrane Lipids in Model Membranes

Larisa Yurlova,[†] Nicoletta Kahya,[‡] Shweta Aggarwal,[†] Hermann-Josef Kaiser,[§] Salvatore Chiantia,[¶] Mostafa Bakhti,[†] Yael Pewzner-Jung,[‖] Oshrit Ben-David,[‖] Anthony H. Futerman,[‖] Britta Brügger,[**] and Mikael Simons[†††*]

[†]Max-Planck-Institute of Experimental Medicine, Göttingen, Germany; [‡]Department of Cell Biology, University Medical Center Groningen, Groningen, The Netherlands; [§]Max-Planck-Institute of Molecular Cell Biology and Genetics, Dresden, Germany; [¶]Department of Biochemistry and Cell Biology, Stony Brook University, Stony Brook, New York; [‖]Department of Biological Chemistry, Weizmann Institute of Science, Rehovot, Israel; [**]Heidelberg University Biochemistry Center, Heidelberg, Germany; and [††]Department of Neurology, University of Göttingen, Göttingen, Germany

ABSTRACT Rapid conduction of nerve impulses requires coating of axons by myelin sheaths, which are multilamellar, lipid-rich membranes produced by oligodendrocytes in the central nervous system. To act as an insulator, myelin has to form a stable and firm membrane structure. In this study, we have analyzed the biophysical properties of myelin membranes prepared from wild-type mice and from mouse mutants that are unable to form stable myelin. Using C-Laurdan and fluorescence correlation spectroscopy, we find that lipids are tightly organized and highly ordered in myelin isolated from wild-type mice, but not from *shiverer* and ceramide synthase 2 null mice. Furthermore, only myelin lipids from wild-type mice laterally segregate into physically distinct lipid phases in giant unilamellar vesicles in a process that requires very long chain glycosphingolipids. Taken together, our findings suggest that oligodendrocytes exploit the potential of lipids to self-segregate to generate a highly ordered membrane for electrical insulation of axons.

INTRODUCTION

The peripheral and the central nervous system of higher vertebrates employs myelin—a membrane produced by the specialized glia, oligodendrocytes, and Schwann cells—to increase the speed at which electrical signals propagate along the axons (1–3). To fulfill this important task, myelin is built as an electrical insulator that increases the electrical resistance and decreases the capacitance across the axon. Consistent with its insulating properties, myelin is produced as a compact, multilayered membrane with a unique molecular composition. Myelin contains a high amount of lipids (~70–80% of dry myelin weight) and is particularly enriched in two glycosphingolipids, namely, galactosylceramide and sulfatide (~28% of dry lipid weight) (4–6).

In addition, myelin comprises a high proportion of cholesterol and large amounts of lipids with saturated long-chain fatty acids, and is also enriched in plasmalogens (etherlipids). During the active phase of myelination, each oligodendrocyte produces as much as ~5–50 $\times$ 10^3 μm^2 of myelin membrane surface area per day (7). The synthesis of myelin starts when oligodendrocyte precursor cells have arrived at their final target, exit the cell-cycle, become nonmigratory, and differentiate into myelin-forming oligodendrocytes (8). This transition is marked by major changes in cell morphology. In culture, oligodendrocytes first generate polarized cellular processes from which they later extend huge amounts of flat membrane sheets. Although continuous with the plasma membrane of the oligodendrocytes, the myelin-membrane composition differs vastly from that of the membrane of the cellular processes and the cell body (9). It is not known how oligodendrocytes create and maintain distinct lipid compositions in these different membrane domains.

In this study, we addressed the mechanisms involved in the generation of these membrane domains. Lipids have the intrinsic property to self-organize; and studies in model membranes have provided evidence that lipid can exist in separate liquid phases. For example, liquid-liquid immiscibility was observed when total lipid extracts from the erythrocyte membrane were spread as monolayer at the air-water interface (10). In contrast, lipid extracts from myelin membrane seems to form homogenous monolayers, when proteins are missing (11–13).

Here, we analyzed the biophysical properties of myelin lipids and examined whether they can segregate from lipids produced by immature oligodendrocytes when reconstituted in artificial model membranes. We speculate that the intrinsic capacity of myelin lipids to self-segregate into a highly ordered phase is an important feature to maintain myelin stability.

MATERIALS AND METHODS

Mouse lines

Ceramide synthase 2 (*CerS2*) null mice were maintained on a mixed C57BL/6 $\times$ 129S4/SvJae background (14,15) and the *shiverer* mice (16) were maintained on a C57/N background. Genotyping of the mice was performed by polymerase chain reaction. For myelin isolation, brains of adult animals ($P \geq 21$) were used, with wild-type littermates serving as controls. For independent analysis (data in Fig. 1), wild-type mice were chosen from an outbred stock.

Submitted March 16, 2011, and accepted for publication October 24, 2011.

*Correspondence: msimons@gwdg.de

Editor: Anne Kenworthy.

0006-3495/11/12/2713/8 $2.00

doi: 10.1016/j.bpj.2011.10.026

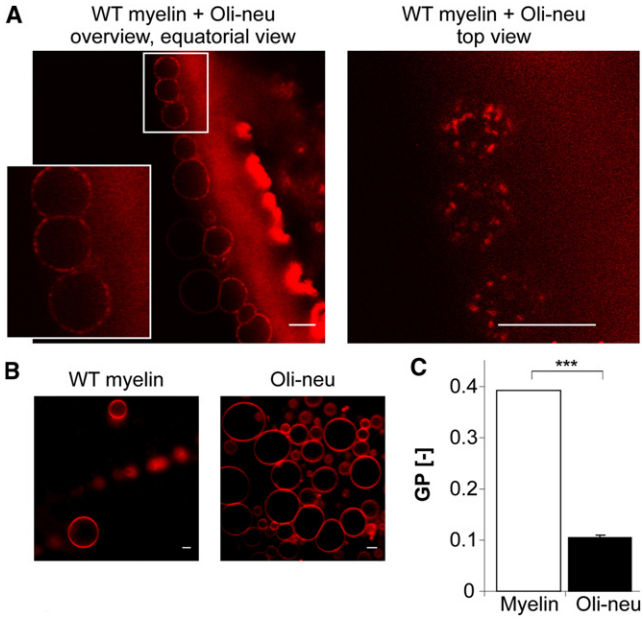

FIGURE 1 Self-segregation of highly ordered myelin lipids results in their lateral heterogeneity in model membranes. (*A*) GUVs were prepared using 1:1 lipid mixtures from total oligodendroglial precursor cell (Oli-neu) membranes and wild-type (WT) myelin. A quantity of 0.1 mol % DiD (*red*) was used to distinguish the lipid phases. Scale bar, 10 μm. (*B*) Control experiments show no domain formation in GUVs prepared from wild-type myelin lipids or from Oli-neu lipids only (with addition of 0.1 mol % DiD (*red*)). Scale bar, 10 μm. (*C*) C-Laurdan spectroscopy reveals much higher lipid order (higher GP [−] values) in purified myelin lipids than in lipid membranes from Oli-neu membranes. (*Bars*) Mean ± SD ($n = 3$, $^{***}p < 0.001$, *t*-test).

Cell culture and treatments

Cell cultures were maintained in humidified 37°C, 7.5% CO_2 incubators. All basal media, supplements, antibiotics, and sera were purchased from Gibco/Invitrogen (Invitrogen, Darmstadt, Germany). The mouse oligodendrocyte precursor cell line Oli-neu (17) was cultured in high-glucose Dulbecco's modified Eagle's medium-based medium containing 5% horse serum, penicillin/streptomycin, glutamax, putrecine, triiodothyronine, L-thyroxine, progesterone, and ITS-A supplement. The cells were grown on polylysine-coated dishes and passaged 1:5 every 2–3 days when grown to ~80% confluence.

Primary cultures of mouse oligodendrocytes were prepared from neonatal mouse brains as reported previously in Trajkovic et al. (18). The oligodendroglial progenitors growing on an astrocyte layer were shaken off and further cultured on polylysine-coated dishes or glass coverslips in high-glucose Dulbecco's modified Eagle's medium-based serum-free medium containing penicillin/streptomycin, glutamax, sodium pyruvate, triiodothyronine, L-thyroxine, and B-27 supplement. To reduce the rate of sphingolipid biosynthesis, oligodendroglial progenitors were cultured in presence of the ceramide synthase inhibitor, fumonisin B1 (Sigma-Aldrich, Munich, Germany). Fumonisin B1 was added to the culture media up to a final concentration 50 μM every 48 h starting from the day of the shake.

Preparation of myelin and total membrane fractions

Crude myelin fractions were prepared from the wild-type and mutant mouse brains according to the classical sucrose gradient centrifugation protocols of Norton and Poduslo with modifications described by Larocca and Norton (19). In brief, brains were homogenized in a hypotonic HE buffer (10 mM HEPES, 5 mM EDTA, supplemented with protease inhibitors, as Complete Mini; Roche Applied Science, Mannheim, Germany) and subjected to centrifugation at 75 000 × *g* for 30 min at 4°C in a sucrose gradient. Crude myelin fractions were collected from 0.32:0.85 M sucrose interface, sedimented by centrifugation at 75,000 × *g* for 30 min at 4°C, washed twice with ice-cold H_2O, and pelleted after each wash by low-speed centrifugation at 12,000 × *g* for 10 min at 4°C.

For the preparation of total membrane fractions, cultured Oli-neu cells were harvested and homogenized in a hypotonic buffer (20 mM Tris/HCl, pH 7.4, 1 mM $MgCl_2$, supplemented with protease inhibitors), and sheared on ice by passing 15 times through a 27 G needle. Nuclei were sedimented by centrifugation at 300 × *g* for 5 min, and total membranes were sedimented from the postnuclear supernatants by centrifugation at 100,000 × *g* for 30 min at 4°C.

Lipid analysis

Lipids were isolated from myelin and total membrane fractions by chloroform-methanol extraction (20). Quantitative analyses of lipids by nano-electrospray ionization tandem mass spectrometry were performed as described in Brügger et al. (21). Lipid analysis was done in positive ion mode on a QII triple quadrupole mass spectrometer (Micromass, Waters, Milford, MA), equipped with a nano Z-spray (22). Cone voltage was set to 30 V. Phosphatidylcholine and sphingomyelin detection was performed by precursor ion scanning for fragment ion 184 Da at a collision energy of 32 eV. Precursor ion scanning of *m/z* 364, 390, and 392 was used for detection of plasmalogen species, employing a collision energy of 20 eV. Hexosylceramide and ceramide were detected by precursor ion scanning for fragment ion 264 Da at a collision energy of 35 eV or 30 eV, respectively. Neutral loss scanning of *m/z* 141 Da, 185 Da, 189 Da, or 277 Da, respectively, was applied for the analyses of phosphatidylethanolamine, phosphatidylserine, phosphatidylglycerol, or phosphatidylinositol, employing a collision energy of 20 eV, except for phosphatidylinositol where a collision energy of 30 eV was applied. Cholesterol was analyzed as an acetate derivate as described in Liebisch et al. (23).

Preparation of giant unilamellar vesicles

For the preparation of giant unilamellar vesicles (GUVs) from complex lipid mixtures, lipids were isolated from myelin fractions and from the total cell membrane fractions by chloroform-methanol extraction (24). For the preparation of GUVs from simple three-component lipid mixtures, 1,2-di-(9Z-octadecenoyl)-*sn*-glycero-3-phosphocholine (DOPC), 3-O-sulfo-β-D-C24:0-galactosylceramide (sGalC(C24)), 3-O-sulfo-β-D-C17:0-galactosylceramide (sGalC(C17)), and 3-O-sulfo-β-D-C12:0-galactosylceramide (sGalC(C12)) were purchased from Avanti Polar Lipids (Alabaster, AL). Cholesterol and chicken egg yolk sphingomyelin (eSM) were obtained from Sigma-Aldrich.

GUVs were reconstituted from equimolar mixtures of lipids (1:1 ratio for the lipid mixtures myelin/oli-neu, 1:1:1 for DOPC/cholesterol/sphingolipid) and 0.1 mol % of DiD (Invitrogen). For the preparation of GUVs, the electroformation method was used, which yields unilamellar vesicles with diameters ranging from 5 to 100 μm (25). The perfusion chamber used for vesicle preparation was equipped with two microscope slides, each coated with indium-tin oxide (Philips, Eindhoven, The Netherlands), which is electrically conductive and exhibits high light transmission in the visible range. GUVs were grown in the perfusion chamber at high temperature (60°C) in the presence of water, as a result of lipid swelling under an AC field (26,27). GUVs were always prepared in the presence of the reducing agent dithiothreitol (2 mM, final concentration), to prevent possible lipid oxidation, which did not affect domain assembly. We did not detect the proteolipid protein in the GUVs preparation using myelin lipid

extracts, as determined by Western blotting. However, small amounts of remaining proteolipid protein cannot be excluded.

Imaging was performed for at least four independent GUV preparations for each lipid mixture. For image acquisition, a DMIRE2 microscope and a TCS SP2 AOBS confocal laser scanning setup (both by Leica Microsystems, Mannheim, Germany) equipped with 40 × NA 1.25 or 63 × NA 1.4 oil Plan-Apochromat objectives were used.

Fluorescence correlation spectroscopy

Translational diffusion coefficients in myelin lipids were estimated with fluorescence correlation spectroscopy (FCS). For this, crude myelin fractions were prepared from the brains of wild-type, *shiverer*, and *CerS2* knockout mice, followed by the lipid extraction according to Folch et al. (24) and GUV electro-formation in water (see above). FCS measurements were then performed as described in Ries et al. (27). Accurate calibration was performed using line-scanning FCS on reference samples (28). The relative diffusion coefficients D for each lipid extract were then calculated as average value in at least 10 vesicles from one or two independent preparations. GUVs were labeled with ~0.005 mol % Bodipy FL Cholesteryl (Molecular Probes, Darmstadt, Germany).

C-Laurdan fluorescence spectroscopy and two-photon microscopy

C-Laurdan spectra from the myelin lipids and total membrane lipid preparations were recorded with 1 nm resolution on a Fluoromax-3 fluorescence spectrometer (Horiba, Kyoto, Japan) at 23°C. All spectra were recorded twice, averaged, and background-subtracted. Excitation wavelengths for C-Laurdan were 385 nm and the generalized polarization (GP) values for C-Laurdan were calculated from the following emission bands: (Ch1) 400–460 nm and (Ch2) 470–530 nm according to Kaiser et al. (29). From the control and fumonisin B1-treated primary oligodendrocytes, C-Laurdan emission was recorded with two-photon microscopy as detailed in Kaiser et al. (29).

Fluorescence recovery after photobleaching

For the fluorescence recovery after photobleaching (FRAP) experiments, control and fumonisin B1-treated primary oligodendrocytes were stained live with CellMask Orange (Invitrogen). Imaging was carried out with a TCS SP2 AOBS confocal laser scanning setup (Leica Microsystems) equipped with 63 × NA 1.4 oil Plan-Apochromat objective. Photobleaching was performed in four scans with the 561 laser at full power within a rectangular region (zoom-in mode). Pre- and postbleach fluorescence intensities (2 and 20 scans, respectively) were monitored with ~25% laser power. Eight-bit images were recorded every 0.657 s at resolution of 512 × 512 pixels, with a scanner speed of 800 Hz. Processing and analysis of FRAP data was performed according to Kenworthy (30).

RESULTS AND DISCUSSION

Myelin contains high levels of saturated, long-chain lipids and is enriched in glycosphingolipids and cholesterol, which together are likely to result in a tightly organized and highly ordered membrane structure (31,32). To assess the lipid order of myelin, we purified myelin from brains of adult mice by discontinuous density gradient centrifugation and recorded the fluorescent spectra of an incorporated C-Laurdan dye in a spectrofluorometer (29). The fluorescent dye C-Laurdan undergoes a shift in its peak emission wavelength from ~500 nm in disordered membranes to 430 nm in condensed membranes. The shift is caused by the increased penetration depth of water into the membrane for disordered bilayers relative to ordered ones. Using C-Laurdan it is, thus, possible to estimate membrane order by acquiring fluorescence in two channels and constructing a normalized ratio image known as a generalized polarization (GP) image (33–35). The overall GP ratio of myelin was high, consistent with it being a highly condensed and ordered membrane (Fig. 1 *C*) (31,32).

For comparison, we isolated membranes from the oligodendroglial precursor cells, Oli-neu, that are arrested in a precursor state and therefore do not synthesize myelin. As expected, the lipid order in total Oli-neu cell membranes was much lower than in myelin (Fig. 1 *C*). We used nanoelectrospray ionization tandem mass spectrometry to characterize the lipid composition of Oli-neu cell membranes and found that these cells contain lower amounts of hexosylceramide, cholesterol, and plasmalogen, but higher amounts of phosphatidylcholine, phosphatidylethanolamine, and phosphatidylinositol as compared to myelin (Fig. 2 *D*). Myelin hexosylceramides were mostly represented by the very long chain lipid species (24:1), whereas the Oli-neu hexosylceramides more often contained shorter acyl chains (16:0) (Fig. 3 *A*). In addition, when further lipid species were analyzed, we observed that in contrast to myelin lipids, the phosphatidylcholine, phosphatidylethanolamine, phosphatidylinositol, and plasmalogens from Oli-neu cells were relatively enriched in poly-unsaturated fatty acids (Fig. 3 *B*, also Fig. S1 in the Supporting Material).

For the formation of myelin, oligodendrocyte precursor cells differentiate into mature oligodendrocytes that synthesize large amounts of myelin lipids. This transition is accompanied by the establishment of cell polarity, i.e., the segregation of myelin from the plasma membrane present in the cellular process and the cell body. Here, we used artificial membranes to model this process.

To test whether the myelin lipids are able to segregate from the lipids of oligodendrocyte precursor cell membranes, experiments with GUVs were performed. Strikingly, when lipids from these two membranes were combined in a 1:1 ratio together with 0.01 mol % DiD, domain formation was clearly observed in most of the GUVs (Fig. 1 *A*). Most vesicles showed domains enriched in DiD coexisting with domains that excluded this dye. GUVs containing only lipids of purified myelin or only lipids of Oli-neu membranes did not show any evidence of lateral segregation (Fig. 1 *B*).

Next, a myelin purification protocol was applied to brains from *shiverer* mice that lack myelin basic protein (MBP) and are unable to form compact myelin. Mass spectrometry revealed that purified myelin from *shiverer* mice contained much lower amounts of hexosylceramides, cholesterol, and plasmalogens and higher amounts of phosphatidylcholine and phosphatidylethanolamine as compared to

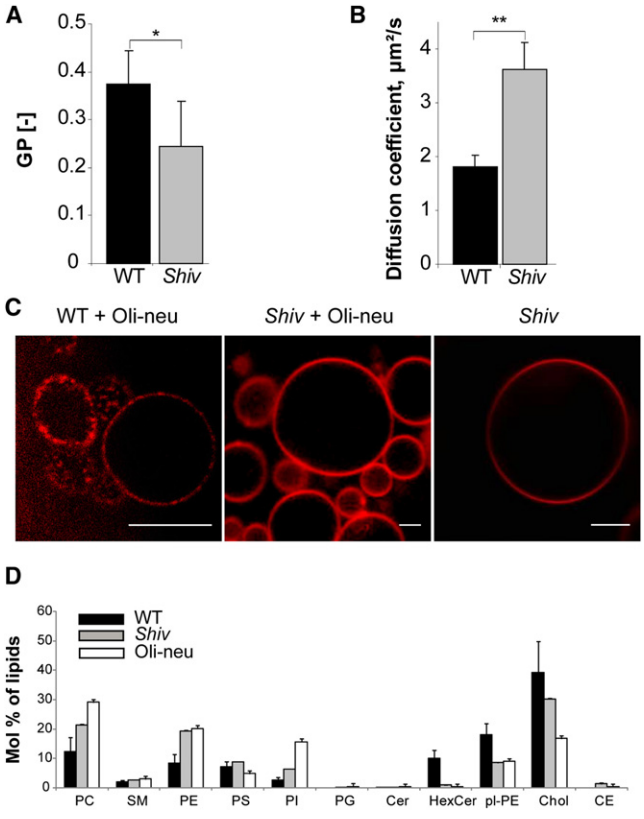

FIGURE 2 *Shiverer* myelin lipid extracts have altered physical properties and do not phase-separate in model membranes. (*A*) C-Laurdan spectroscopy showed reduced lipid order in myelin lipids from *shiverer* mice (*Shiv*) as compared to wild-type (WT) myelin lipid extracts. (*Bars*) Mean ± SD ($n = 6$, $^*p < 0.05$, *t*-test). (*B*) FCS measurements reveal increase in lipid translational diffusion rate in lipids extracted from *shiverer* myelin compared to wild-type myelin. (*Bars*) Mean ± SD ($n = 8$–10, $^{**}p < 0.01$, *t*-test). (*C*) Lateral segregation was only observed when WT myelin was mixed with lipids from Oli-neu membranes, but not when lipids from myelin of *shiverer* were used. A quantity of 0.1 mol % DiD (*red*) was used to mark lipid domains. Scale bar, 10 μm. (*D*) Lipid analyses of WT myelin, *shiverer* myelin (*Shiv*), and of total membrane preparations from oligodendroglial precursor cells (Oli-neu). The following lipid classes are shown: *PC*, phosphatidylcholine; *SM*, sphingomyelin; *PE*, phosphatidylethanolamine; *PS*, phosphatidylserine; *PI*, phosphatidylinositol; *PG*, phosphatidylglycerol; *Cer*, ceramide; *HexCer*, hexosylceramide; *pl-PE*, plasmenylethanolamine (plasmalogen PE); *Chol*, cholesterol; and *CE*, cholesterol esters. (*Graph bars*) Mean ± SD from three experiments.

wild-type myelin (Fig. 2 *D* (36)). In addition, phosphatidylcholine, phosphatidylinositol, phosphatidylethanolamine, phosphatidylserine, and plasmalogens from *shiverer* preparations contained more poly-unsaturated fatty acids than those from the wild-type preparations (Fig. 3 *B*; see also Fig. S1). Furthermore, when lipids from *shiverer* mice were mixed with oligodendroglial cell membrane lipids in GUVs, domains did not form (Fig. 2 *C*).

To analyze the membrane organization of myelin from *shiverer* mice, C-Laurdan and fluorescence correlation spectroscopy (FCS) measurements were performed. These experiments revealed a decrease in lipid order and an increase in lipid translational diffusion in purified myelin from mice lacking MBP as compared to myelin from wild-type mice (Fig. 2, *A* and *B*). Together these results suggest that the specific lipid composition of compact myelin provides high membrane order and drives phase-separation. Very long chain glycosphingolipids are possible candidates. A key enzyme in their biosynthesis is ceramide synthase 2.

Ceramide synthase 2 (*CerS2*) null mice exhibit strongly reduced levels of ceramide species with very long fatty acid residues ($\geq$ C22) in the brain and a severe decrease in the amount of galactosylceramides and sulfatides in the myelin membrane (37). Consequently, from early adulthood on, myelin stability is progressively lost and accompanied by loss of compacted myelin. Having shown the ability of stable wild-type myelin lipids to laterally segregate and form a distinct lipid phase in GUVs, we next asked whether the myelin-enriched sphingolipids, galactosylceramides/sulfatides with very long chain fatty acids, are required for this process. Therefore, we tested whether myelin prepared from ceramide synthase 2 null mice (14,15) is able to self-segregate into domains in GUVs.

When lipid extracts from *CerS2* null myelin and from immature oligodendroglial membranes were combined, the distribution of lipids remained homogenous and domains did not form (Fig. 4 *C*). Furthermore, C-Laurdan and FCS measurements showed that myelin lipids purified from *CerS2* null mice are less condensed as compared to myelin lipids from wild-type littermates (Fig. 4, *A* and *B*). These experiments, thus, indicate that very long chain fatty acid containing glycosphingolipids play an instrumental role in organizing domains in oligodendroglial model membranes.

We could further confirm that glycosphingolipids are crucial for the high myelin membrane order and for the lateral segregation processes in a series of cell culture and in vitro experiments. Cultivating mouse primary oligodendrocytes in presence of the inhibitor of ceramide synthesis, fumonisin B1, led to a decrease in the membrane order and an increase in the diffusion rate in their plasma membranes, as measured with C-Laurdan 2-photon microscopy and FRAP, respectively (Fig. 5, *A*–*C*). These effects may be due to the depletion of glycosphingolipids, but indirect effects of fumonisin B1 on the cells cannot be excluded. Moreover, in GUVs generated from simple mixtures of synthetic lipids, domain formation was only observed when DOPC, cholesterol, and sulfogalactosylceramide sGalC(C24) or (C17), but not the short-chain sulfogalactosylceramide sGalC(C12), were combined (Fig. 5 *D*).

Together, our findings show that myelin lipids are highly ordered and can self-organize in a process that requires glycosphingolipids. In contrast to many biophysical studies, which focus on well-defined two- and three-component model membranes, we used complex mixtures of lipids from native membranes. We compared the biophysical

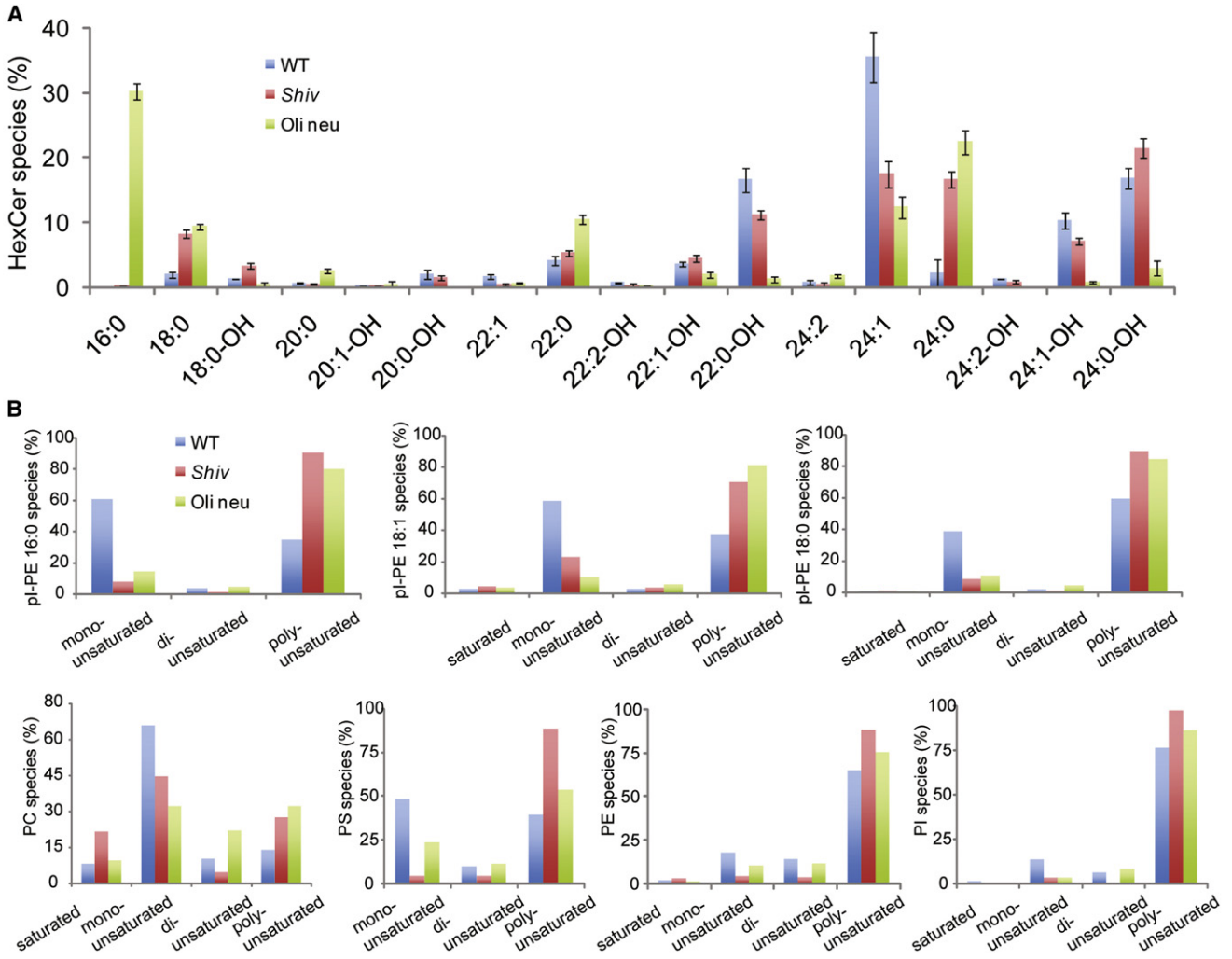

FIGURE 3 Analyses of fatty acid chains in lipids from wild-type (WT) myelin, *shiverer* myelin (*Shiv*), and from membrane preparations from Oli-neu cells (Oli-neu). Abbreviations of the lipid classes are in the legend to Fig. 2 *D*. (*A*) Acyl-chain profiling of hexosylceramides (HexCer). (*Graph bars*) Mean ± SD from three experiments. Note that most HexCers in Oli-neu membranes contain a 16:0 acyl chain, whereas a much longer 24:1 fatty acid is predominantly used for HexCers in WT myelin. (*B*) Summary of the saturation analysis of acyl chains in different lipid classes (for detailed analysis, see Fig. S1 in the Supporting Material).

properties of myelin lipids from wild-type mice to those from mouse mutants that do not form stable myelin. The differences were striking. Lipids from wild-type myelin were highly ordered and able to segregate from a mixture of less ordered lipids from oligodendrocyte precursor cells. This was not the case for myelin lipids purified from *shiverer* mice or from *CerS2* null mice, which are deficient in ceramide species with very long fatty acid residues.

Our study shows that despite its compositional complexity, myelin lipids have an intrinsic ability to phase-separate, which critically depends on glycosphingolipids with very long acyl chains. Cholesterol, which is also found in high amounts in myelin, is likely to play an essential role as well. The important role of cholesterol in myelin-membrane growth is nicely illustrated in mutant mice that lack the ability to synthesize cholesterol in myelin-forming oligodendrocytes (conditional inactivation of squalene synthase gene (*Fdft1*) in oligodendrocytes) (38). These mice form small amounts of myelin, but compensate the lack of endogenous cholesterol biosynthesis by taking up cholesterol from an external source.

Selective incorporation of long fatty acids into sphingolipids seems to be conserved among eukaryotes and was also shown to support phase segregation in yeast lipid extracts (39). Our findings correlate well with the previously reported ability of long-chain lipids to stabilize lipid domains by increasing the line tension (40). We did not focus on asymmetry across lipid bilayer in this study, although this is likely to contribute to myelin membrane organization. For example, interdigitation of very long chain lipids into the cytoplasmic leaflet may also play a role in membrane domain formation (41). On the other hand, we

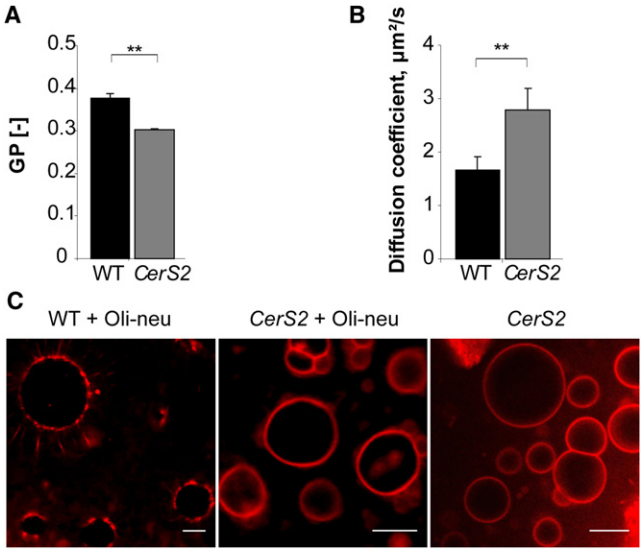

FIGURE 4 Lack of very long-chain sphingolipids decreases myelin lipid order and prevents lateral segregation of myelin lipids in model membranes. (*A*) C-Laurdan fluorescence spectroscopy shows significantly lower GP [−] values in myelin lipid fractions, prepared from *CerS2* null mice (*CerS2*) as compared to myelin lipids isolated from the wild-type (WT) littermate controls (*t*-test; **, $p < 0.01$; $n = 3$). (*Bars*) Mean ± SD. (*B*) FCS measurements show increase in lipid translational diffusion in purified myelin lipids from *CerS2* null mice compared to WT littermates (*t*-test; **, $p < 0.01$; $n = 8$). (*Bars*) Mean values ± SD. (*C*) GUVs were prepared using 1:1 lipid mixtures from total Oli-neu membranes and wild-type or mutant myelin (*CerS2* null mice). Lateral segregation was not observed when lipids from myelin of *CerS2* null mice were used. The value 0.1 mol % DiD (*red*) was used to distinguish lipid phases. Scale bar, 10 μm.

cannot exclude that a loss of bilayer asymmetry might reinforce the microscopic segregation that we observed in this study. Experiments exploiting the newly established methods to produce asymmetric GUVs will be important to clarify this aspect in future studies (42). Nevertheless, our results clearly show that wild-type myelin lipids have to be mixed with lipids from a less ordered membrane (Oli-neu cells) to observe microscopic lateral segregation of lipids in GUVs.

These findings concur with classical x-ray scattering studies of myelin membrane structure (31). Whereas these results provide evidence for a highly ordered homogenous state of the lipids in the bulk of myelin, other studies using different methods have observed lateral structural heterogeneities within myelin. For example, previously reported experiments using myelin extracts reconstituted in monolayers at the air-water interface demonstrate phase domain microheterogeneity over the whole compression isotherm (43,44). Interestingly, incorporation of myelin basic protein or the proteolipid protein into the monolayer promoted lateral segregation (45). Recently, monolayers based on the lipid composition of normal myelin and on the composition of white matter from marmosets with experimental allergic encephalomyelitis showed that this system was able to visualize differences in phase behavior due to subtle lipid alterations (46).

Whereas phase separation has been shown to occur in model membranes in vitro, the situation in cellular membranes is still a subject of debate (47,48). In cell membranes, large-scale phase separation has only been observed when large membrane blebs (giant membrane vesicles) are artificially induced (49,50). Cellular membranes are crowded with proteins, which could exert distorting effects preventing self-organization of lipids within a membrane (51). In addition, cellular membranes are extremely dynamic structures, which are constantly exchanging molecules and rapidly renew their structure by processes such as endo- and exocytosis. The situation is different in myelinating glia. Myelin is a metabolically relatively stable lipid-rich membrane with a slow turnover rate, which contains very little protein and high amounts of galactosylceramide/sulfatide with very long chain fatty acids (52). These features may have enabled the myelin-producing cells, oligodendrocytes, to exploit the physical properties of membrane lipids to self-organize. We suggest that this self-organization contributes to the assembly of stable myelin in vivo. Whether this is solely dependent on lipids or if proteins are also involved in phase separation remains to be seen.

One candidate protein is MBP itself. MBP is highly positively charged and binds electrostatically to the negatively charged cytoplasmic membrane surfaces. There is also a putative α-helix segment of MBP at the N-terminus that can partially penetrate into the lipid layer and thereby expands the cytoplasmic leaflet of the myelin membrane (53). The interaction of MBP to the membrane is known to contribute to plasma membrane lipid organization and the lateral segregation of lipids (11,54–57). Another important function of MBP is to set up a fence along the growing myelin sheath to form a barrier, which restricts the entry of proteins with large cytoplasmic domains into the membrane sheets (58). This barrier acts as a molecular sieve that is impermeable for most proteins, but not for lipids, and thus is a precondition for the formation of a lipid-rich membrane. MBP, thus, appears to have a dual function: to form a diffusion barrier for proteins and to organize myelin membrane lipids. These mechanisms of myelin biogenesis might have evolved as the generation of a condensed membrane with highly ordered lipids is a prerequisite for myelin to fulfill its function as an electrical insulator.

The biophysical methods that were employed in this study proved to be applicable for the analysis of the myelin membrane properties and will be useful in the characterization of myelin mouse mutants in future research.

CONCLUSIONS

Oligodendrocytes synthesize large amounts of cellular membrane to form multiple myelin internodes of highly

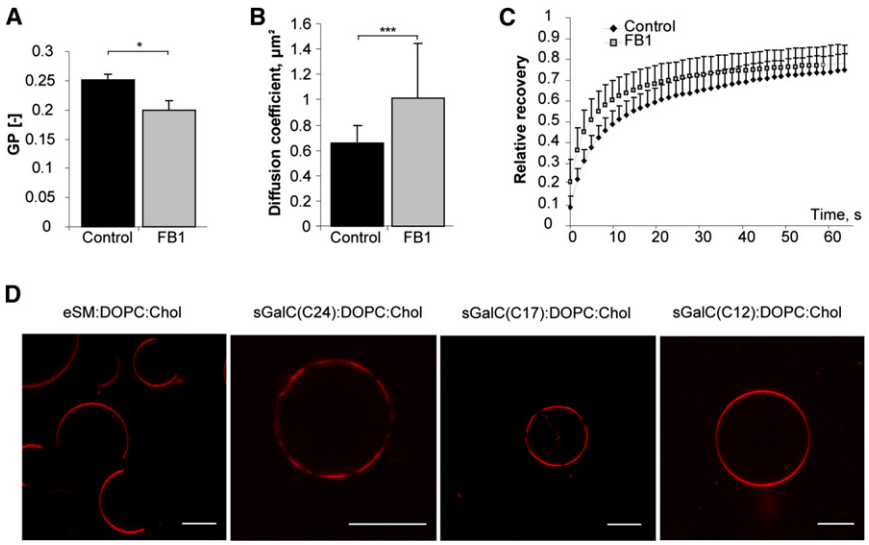

FIGURE 5 (*A–C*) Depletion of sphingolipids decreases membrane order and increases the diffusion rate in myelinlike membrane sheets of primary oligodendrocytes. Values are mean ± SD. (*A*) C-Laurdan two-photon microscopy reveals decrease in GP [−] values in myelinlike sheets of primary oligodendrocytes treated with fumonisin B1 (*t*-test, *, $p < 0.05$; $n = 3$). (*B*) Fluorescence recovery after photobleaching shows an increase in the diffusion coefficient of the amphipathic plasma membrane stain, CellMask Orange, in the membrane of live primary oligodendrocytes after fumonisin B1 treatment (*t*-test, ***, $p < 0.001$; $n = 26–30$). (*C*) FRAP time-dependent recovery curves of CellMask Orange in control and fumonisin B1-treated primary oligodendrocytes. (*D*) GUVs were prepared from equimolar mixtures of synthetic lipids; 0.1 mol % Rhodamine-labeled DPPE was used to mark the disordered phase; images were acquired with a confocal microscope. Phase separation can be easily observed in the majority of GUVs composed of eSM/DOPC/Cholesterol, sGalC(C24)/DOPC/Cholesterol or sGalC(C17)/DOPC/Cholesterol, but not when the shorter chain sphingolipid was used, as in sGalC(C12)/DOPC/Cholesterol. Scale bar, 10 μm.

stable membranes with a specific set of highly ordered lipids. In this study, we demonstrate that in model membranes myelin lipids self-organize and segregate when combined with the lipids produced by oligodendrocyte precursor cells. By employing mouse mutants that are unable to form stable myelin, we deciphered a critical role of very long chain glycosphingolipids in this process.

In addition, using C-Laurdan and FCS we found that myelin membrane isolated from *shiverer* and *CerS2* null mice that do not produce very long chain glycosphingolipids is not as tightly organized and contains more loosely packed lipids than the ones isolated from wild-type mice. *CerS2* null mice that lack long-chain ceramide species provide evidence that the high lipid order is likely to be essential for long-term maintenance of myelin stability (37). We suggest that oligodendrocytes exploit the potential of lipids to self-segregate to generate a highly ordered myelin membrane for electrical insulation of axons. The biophysical methods used in this study will be highly relevant for the analysis of mouse mutants or de- and dysmyelinating diseases, in which myelin stability is compromised.

SUPPORTING MATERIAL

One figure is available at http://www.biophysj.org/biophysj/supplemental/S0006-3495(11)01247-1.

L.Y. was supported by a Neurest Marie Curie Stipend, and L.Y. and S.A. were also supported by the International Max Planck Research School, MSc/PhD Molecular Biology Program. S.C. is a Howard Hughes Medical Institute fellow of the Life Sciences Research Foundation. This work was supported by a European Research Council Starting Grant (to M.S.), the European Molecular Biology Organization Young Investigator Program (to M.S.), and Sonderforschungsbereich/Transregio8 (to B.B.).

REFERENCES

1. Sherman, D. L., and P. J. Brophy. 2005. Mechanisms of axon ensheathment and myelin growth. *Nat. Rev. Neurosci.* 6:683–690.
2. Simons, M., and J. Trotter. 2007. Wrapping it up: the cell biology of myelination. *Curr. Opin. Neurobiol.* 17:533–540.
3. Zalc, B., D. Goujet, and D. Colman. 2008. The origin of the myelination program in vertebrates. *Curr. Biol.* 18:R511–R512.
4. Baumann, N., and D. Pham-Dinh. 2001. Biology of oligodendrocyte and myelin in the mammalian central nervous system. *Physiol. Rev.* 81:871–927.
5. Chrast, R., G. Saher, …, M. H. Verheijen. 2011. Lipid metabolism in myelinating glial cells: lessons from human inherited disorders and mouse models. *J. Lipid Res.* 52:419–434.
6. Jackman, N., A. Ishii, and R. Bansal. 2009. Oligodendrocyte development and myelin biogenesis: parsing out the roles of glycosphingolipids. *Physiology (Bethesda).* 24:290–297.
7. Pfeiffer, S. E., A. E. Warrington, and R. Bansal. 1993. The oligodendrocyte and its many cellular processes. *Trends Cell Biol.* 3:191–197.
8. Emery, B. 2010. Regulation of oligodendrocyte differentiation and myelination. *Science.* 330:779–782.
9. Baron, W., and D. Hoekstra. 2010. On the biogenesis of myelin membranes: sorting, trafficking and cell polarity. *FEBS Lett.* 584:1760–1770.
10. Keller, S. L., W. H. Pitscher, III, …, H. M. McConnell. 1998. Red blood cell lipids form immiscible liquids. *Phys. Rev. Lett.* 81:5019–5022.
11. Rosetti, C. M., R. G. Oliveira, and B. Maggio. 2005. The Folch-Lees proteolipid induces phase coexistence and transverse reorganization of lateral domains in myelin monolayers. *Biochim. Biophys. Acta.* 1668:75–86.
12. Rosetti, C. M., B. Maggio, and N. Wilke. 2010. Micron-scale phase segregation in lipid monolayers induced by myelin basic protein in the presence of a cholesterol analog. *Biochim. Biophys. Acta.* 1798:498–505.

13. Hu, Y., and J. Israelachvili. 2008. Lateral reorganization of myelin lipid domains by myelin basic protein studied at the air-water interface. *Colloids Surf. B Biointerfaces.* 62:22–30.

14. Pewzner-Jung, Y., H. Park, …, A. H. Futerman. 2010. A critical role for ceramide synthase 2 in liver homeostasis. I. Alterations in lipid metabolic pathways. *J. Biol. Chem.* 285:10902–10910.

15. Pewzner-Jung, Y., O. Brenner, …, A. H. Futerman. 2010. A critical role for ceramide synthase 2 in liver homeostasis. II. Insights into molecular changes leading to hepatopathy. *J. Biol. Chem.* 285:10911–10923.

16. Chernoff, G. F. 1981. *Shiverer*: an autosomal recessive mutant mouse with myelin deficiency. *J. Hered.* 72:128.

17. Jung, M., A. J. Crang, …, J. Trotter. 1994. In vitro and in vivo characterization of glial cells immortalized with a temperature sensitive SV40 T antigen-containing retrovirus. *J. Neurosci. Res.* 37:182–196.

18. Trajkovic, K., A. S. Dhaunchak, …, M. Simons. 2006. Neuron to glia signaling triggers myelin membrane exocytosis from endosomal storage sites. *J. Cell Biol.* 172:937–948.

19. Larocca, J. N., and W. T. Norton. 2007. Isolation of myelin. *Curr. Protoc. Cell Biol.* DOI:10.1002/0471143030.cb0325s33.

20. Bligh, E. G., and W. J. Dyer. 1959. A rapid method of total lipid extraction and purification. *Can. J. Biochem. Physiol.* 37:911–917.

21. Brügger, B., B. Glass, …, H. G. Kräusslich. 2006. The HIV lipidome: a raft with an unusual composition. *Proc. Natl. Acad. Sci. USA.* 103:2641–2646.

22. Brügger, B., R. Sandhoff, …, F. T. Wieland. 2000. Evidence for segregation of sphingomyelin and cholesterol during formation of COPI-coated vesicles. *J. Cell Biol.* 151:507–518.

23. Liebisch, G., M. Binder, …, G. Schmitz. 2006. High throughput quantification of cholesterol and cholesteryl ester by electrospray ionization tandem mass spectrometry (ESI-MS/MS). *Biochim. Biophys. Acta.* 1761:121–128.

24. Folch, J., M. Lees, and G. H. Sloane Stanley. 1957. A simple method for the isolation and purification of total lipids from animal tissues. *J. Biol. Chem.* 226:497–509.

25. Kahya, N., D. Scherfeld, and P. Schwille. 2005. Differential lipid packing abilities and dynamics in giant unilamellar vesicles composed of short-chain saturated glycerol-phospholipids, sphingomyelin and cholesterol. *Chem. Phys. Lipids.* 135:169–180.

26. García-Sáez, A. J., and P. Schwille. 2010. Stability of lipid domains. *FEBS Lett.* 584:1653–1658.

27. Ries, J., S. R. Yu, …, P. Schwille. 2009. Modular scanning FCS quantifies receptor-ligand interactions in living multicellular organisms. *Nat. Methods.* 6:643–645.

28. Kahya, N., D. Scherfeld, …, P. Schwille. 2003. Probing lipid mobility of raft-exhibiting model membranes by fluorescence correlation spectroscopy. *J. Biol. Chem.* 278:28109–28115.

29. Kaiser, H. J., D. Lingwood, …, K. Simons. 2009. Order of lipid phases in model and plasma membranes. *Proc. Natl. Acad. Sci. USA.* 106:16645–16650.

30. Kenworthy, A. K. 2007. Fluorescence recovery after photobleaching studies of lipid rafts. *Methods Mol. Biol.* 398:179–192.

31. Franks, N. P., V. Melchior, …, D. L. Caspar. 1982. Structure of myelin lipid bilayers. Changes during maturation. *J. Mol. Biol.* 155:133–153.

32. Oliveira, R. G., R. O. Calderón, and B. Maggio. 1998. Surface behavior of myelin monolayers. *Biochim. Biophys. Acta.* 1370:127–137.

33. Parasassi, T., G. De Stasio, …, E. Gratton. 1990. Phase fluctuation in phospholipid membranes revealed by Laurdan fluorescence. *Biophys. J.* 57:1179–1186.

34. Gaus, K., E. Gratton, …, W. Jessup. 2003. Visualizing lipid structure and raft domains in living cells with two-photon microscopy. *Proc. Natl. Acad. Sci. USA.* 100:15554–15559.

35. Owen, D. M., A. Magenau, …, K. Gaus. 2010. Imaging membrane lipid order in whole, living vertebrate organisms. *Biophys. J.* 99:L7–L9.

36. Bird, T. D., D. F. Farrell, and S. M. Sumi. 1978. Brain lipid composition of the *Shiverer* mouse: (genetic defect in myelin development). *J. Neurochem.* 31:387–391.

37. Imgrund, S., D. Hartmann, …, K. Willecke. 2009. Adult ceramide synthase 2 (CERS2)-deficient mice exhibit myelin sheath defects, cerebellar degeneration, and hepatocarcinomas. *J. Biol. Chem.* 284:33549–33560.

38. Saher, G., B. Brügger, …, K. A. Nave. 2005. High cholesterol level is essential for myelin membrane growth. *Nat. Neurosci.* 8:468–475.

39. Klose, C., C. S. Ejsing, …, K. Simons. 2010. Yeast lipids can phase-separate into micrometer-scale membrane domains. *J. Biol. Chem.* 285:30224–30232.

40. García-Sáez, A. J., S. Chiantia, and P. Schwille. 2007. Effect of line tension on the lateral organization of lipid membranes. *J. Biol. Chem.* 282:33537–33544.

41. Pinto, S. N., L. C. Silva, …, M. Prieto. 2008. Membrane domain formation, interdigitation, and morphological alterations induced by the very long chain asymmetric C24:1 ceramide. *Biophys. J.* 95:2867–2879.

42. Chiantia, S., P. Schwille, …, E. London. 2011. Asymmetric GUVs prepared by MβCD-mediated lipid exchange: an FCS study. *Biophys. J.* 100:L1–L3.

43. Oliveira, R. G., and B. Maggio. 2000. Epifluorescence microscopy of surface domain microheterogeneity in myelin monolayers at the air-water interface. *Neurochem. Res.* 25:77–86.

44. Oliveira, R. G., and B. Maggio. 2002. Compositional domain immiscibility in whole myelin monolayers at the air-water interface and Langmuir-Blodgett films. *Biochim. Biophys. Acta.* 1561:238–250.

45. Rosetti, C. M., B. Maggio, and R. G. Oliveira. 2008. The self-organization of lipids and proteins of myelin at the membrane interface. Molecular factors underlying the microheterogeneity of domain segregation. *Biochim. Biophys. Acta.* 1778:1665–1675.

46. Min, Y., T. F. Alig, …, J. A. Zasadzinski. 2011. Critical and off-critical miscibility transitions in model extracellular and cytoplasmic myelin lipid monolayers. *Biophys. J.* 100:1490–1498.

47. McConnell, H. M., and M. Vrljic. 2003. Liquid-liquid immiscibility in membranes. *Annu. Rev. Biophys. Biomol. Struct.* 32:469–492.

48. Bagatolli, L. A., J. H. Ipsen, …, O. G. Mouritsen. 2010. An outlook on organization of lipids in membranes: searching for a realistic connection with the organization of biological membranes. *Prog. Lipid Res.* 49:378–389.

49. Baumgart, T., A. T. Hammond, …, W. W. Webb. 2007. Large-scale fluid/fluid phase separation of proteins and lipids in giant plasma membrane vesicles. *Proc. Natl. Acad. Sci. USA.* 104:3165–3170.

50. Lingwood, D., J. Ries, …, K. Simons. 2008. Plasma membranes are poised for activation of raft phase coalescence at physiological temperature. *Proc. Natl. Acad. Sci. USA.* 105:10005–10010.

51. Ryan, T. A., J. Myers, …, W. W. Webb. 1988. Molecular crowding on the cell surface. *Science.* 239:61–64.

52. Aggarwal, S., L. Yurlova, and M. Simons. 2011. Central nervous system myelin: structure, synthesis and assembly. *Trends Cell Biol.* 21:585–593.

53. Harauz, G., V. Ladizhansky, and J. M. Boggs. 2009. Structural polymorphism and multifunctionality of myelin basic protein. *Biochemistry.* 48:8094–8104.

54. Mueller, H., H. J. Butt, and E. Bamberg. 1999. Force measurements on myelin basic protein adsorbed to mica and lipid bilayer surfaces done with the atomic force microscope. *Biophys. J.* 76:1072–1079.

55. Rosetti, C. M., and B. Maggio. 2007. Protein-induced surface structuring in myelin membrane monolayers. *Biophys. J.* 93:4254–4267.

56. Rispoli, P., R. Carzino, …, R. Rolandi. 2007. A thermodynamic and structural study of myelin basic protein in lipid membrane models. *Biophys. J.* 93:1999–2010.

57. Fitzner, D., A. Schneider, …, M. Simons. 2006. Myelin basic protein-dependent plasma membrane reorganization in the formation of myelin. *EMBO J.* 25:5037–5048.

58. Aggarwal, S., L. Yurlova, …, M. Simons. 2011. A size barrier limits protein diffusion at the cell surface to generate lipid-rich myelin-membrane sheets. *Dev. Cell.* 21:445–456.